

Multi-task Manipulation Policy Modeling with Visuomotor Latent Diffusion

Wenhui Tan^{1†}, Bei Liu², Junbo Zhang³,

Ruihua Song^{1‡}, and Jianlong Fu^{2§}

¹ Gaoling School of Artificial Intelligence, Renmin University, China

² Microsoft Research

³ Tsinghua University, China

{tanwenhui404, rsong}@ruc.edu.cn {Bei.Liu, jianf}@microsoft.com
zhangjb21@mails.tsinghua.edu.cn

Abstract. Modeling a generalized visuomotor policy has been a long-standing challenge for both computer vision and robotics communities. Existing approaches often fail to efficiently leverage cross-dataset resources or rely on heavy Vision-Language models, which require substantial computational resources, thereby limiting their multi-task performance and application potential. In this paper, we introduce a novel paradigm that effectively utilizes latent modeling of manipulation skills and an efficient visuomotor latent diffusion policy, which enhances the utilizing of existing cross-embodiment and cross-environment datasets, thereby improving multi-task capabilities. Our methodology consists of two decoupled phases: action modeling and policy modeling. Firstly, we introduce a task-agnostic, embodiment-aware trajectory latent autoencoder for unified action skills modeling. This step condenses action data and observation into a condensed latent space, effectively benefiting from large-scale cross-datasets. Secondly, we propose to use a visuomotor latent diffusion policy that recovers target skill latent from noises for effective task execution. We conducted extensive experiments on two widely used benchmarks, and the results demonstrate the effectiveness of our proposed paradigms on multi-tasking and pre-training. Code is available at <https://github.com/AlbertTan404/RoLD>.

Keywords: Multi-task Robot Manipulation · Diffusion Models · Robotics Pre-training

1 Introduction

The challenge of multi-task visuomotor policy modeling has long been a topic of interest within the fields of computer vision and robotics. In practical terms,

[†] This work was performed when Wenhui Tan and Junbo Zhang were visiting Microsoft Research as research interns.

[‡] Corresponding author.

[§] Corresponding author.

training these types of policies can be conceptualized as imitation learning from demonstrations, necessitating parallel data on observations, task conditions, and actions. Drawing inspiration from the considerable success of pre-training on large-scale datasets in the areas of Computer Vision (CV) [8,25], Natural Language Processing (NLP) [33,45,52], and Vision-Language (VL) [35,1,24,50,22], it becomes clear that a viable strategy towards achieving a generalizable multi-task visuomotor policy is to utilize multiple robotics datasets.

However, the heterogeneity inherent in robotics datasets poses a significant obstacle to effective joint training. Within datasets of the same embodiment, elements such as environments and camera frames may undergo substantial changes. This leads to an unpredictable mapping between action signals and the real actions executed by different robots, and vice versa. When considering datasets of different embodiments [34,10,3,7], the action space can vary dramatically, with some datasets featuring action spaces that are purely movement-based, devoid of rotation or gripper action. Efforts to tackle these challenges have led to the development of frameworks aimed at creating more resilient and universal visuomotor policies. These efforts encompass research in model design [17,42,14,23,3] and training paradigms [21,36,9,48], with the goal of enhancing the efficiency and stability of policy learning. The pioneering work of DiffusionPolicy [6] introduced a diffusion-based policy model, showcasing stable learning of a gradient field for action trajectory prediction. However, DiffusionPolicy primarily focuses on single-task performance and directly learns high-dimensional action sequences, neglecting action space modeling. ACT [51] proposed integrating a generative model for trajectory prediction, along with a chunking mechanism for consistent action execution. Despite this, the framework lacks in disentangling action modeling from policy modeling, impacting its multitasking efficiency. LISA [11], similar to us, involves a two-stage architecture for learning skill representations using the Vector Quantization (VQ) method and constructing a policy model for action prediction. In contrast to LISA, we aim to develop a more precise and robust trajectory latent space by employing latent diffusion policy with cross-embodiment pre-training. Another significant strategy involves large VL models [2,34,38,19], leveraging internet-scale pre-trained models. While these models contain a vast amount of diverse knowledge applicable to manipulation tasks, their considerable size surpasses that of conventional manipulation policy models, limiting their practicality for real-time inference.

Despite these complexities, we contend that action trajectory modeling, in contrast to single-step action prediction, possesses an inherently uniform representation with embedded semantics such as “placing” or “picking”. A well-modeled, uniform action trajectory space is a prerequisite for a general manipulation policy.

Addressing the aforementioned challenges, we propose a novel approach that efficiently models action trajectories within a latent space and further applies latent diffusion for effective policy learning, namely RoLD (**R**obot **L**atent **D**iffusion Policy). Our methodology commences with modeling a compact, embodiment-aware latent action space utilizing an embodiment-aware autoencoder which

enables the efficient compression of diverse action sequences of different embodiments into a compact latent space. We do not instill any task-relevant information in this phase for pure action latent space modeling. In the subsequent phase, we employ latent diffusion on the learned space conditioned on task instructions and observations, thereby facilitating multi-task policy modeling. We first sample from a Gaussian distribution in the latent space, then a latent denoising diffusion process autoregressively recovers the noise to the encoded latent, which is then fed to the decoder for action trajectory prediction. By adopting this approach, we are able to leverage the benefits of diverse robotics datasets for general-purpose training. Simultaneously, our model harnesses the power of diffusion for stable and precise latent predictions. This dual advantage allows us to effectively navigate the complexities of multi-task policy learning in the field of robotics, thereby opening new avenues for exploration and advancement in this domain.

In summary, our contributions are:

- We present uniform trajectory modeling to condense a variety of action sequences into a compact latent space with rich skill-level semantics, enabling effective pre-training across large scale datasets.
- We introduce a Visuomotor Latent Diffusion Policy which stably denoises from a latent trajectory space conditioned by task indicators and observations to enable multi-task manipulation.
- We conduct extensive experiments and reveal that our approach outperforms existing baselines by significant margins of 14% and 24% on two multi-task benchmarks, underscoring the robustness of its multi-task capabilities.

2 Related Works

2.1 Visuomotor Policy Learning

The genesis of vision-based robot control is rooted in Image-Based Visual Servoing (IBVS) [4,31], which predominantly utilized manually crafted algorithms. In contemporary research, the focus has shifted towards learning-based visuomotor policies, now the dominant paradigm. A significant line of inquiry within this domain encompasses Reinforcement Learning (RL) based approaches [5,43,12,53], which integrate policy modeling with RL to notable effect. Despite their advancements, these methods often grapple with challenges such as training inefficiencies and constrained generalization—typical impediments associated with RL. Conversely, the current vanguard of visuomotor policy learning is epitomized by methods that capitalize on learning from expert demonstrations [3,2,38,19,42,27,47] or benefit from real-world videos [29,32,37,46]. This paradigm has demonstrated remarkable training efficiency and precision across both simulated and real-world environments. Our work is aligned with this approach, aiming to harness the potential of cross-dataset joint training.

2.2 Imitation Learning for Robot Manipulation

Imitation learning transcends mere replication of expert demonstrations by striving to apprehend the expert’s underlying strategies. As generative models have progressed in computer vision (CV) and natural language processing (NLP) [13,20,16,39], a new wave of generative approaches has emerged for imitation learning in robot manipulation [18,23,51,9,41]. Notably, Chi et al. [6] utilized a diffusion model to engineer a gradient field conducive to manipulation policy modeling, achieving commendable stability and efficacy. However, it is crucial to recognize that these methods frequently prioritize single-task proficiency at the expense of multitasking versatility. For instance, Zhao et al. [51] leveraged a variational autoencoder for trajectory prediction, followed by action chunking to enhance action execution. Additionally, Garg et al. [11] employed a Vector Quantization technique within the policy model’s bottleneck, facilitating a dual-phase policy modeling approach. These innovative contributions underscore the untapped potential in this arena, especially regarding the adoption of generative models to elevate multitask policy learning capabilities. Pursuing this direction could yield more adaptable and sophisticated visuomotor policies, adept at a wider array of tasks and environments.

2.3 Diffusion Models

Denoising diffusion probabilistic models (DDPM) [16] have recently risen to prominence, rivalling the sample generation prowess of Generative Adversarial Networks (GANs) [13] and Variational Autoencoders (VAEs) [20]. The DDPM framework conceptualizes data generation as a diffusion process, thereby offering a distinct perspective on model formulation. Nichol et al. [39] introduced Latent Diffusion Models (LDM), which amalgamate the merits of VAEs and diffusion models. This innovation involves conducting the diffusion process within a latent space, as opposed to the conventional pixel space, which not only enhances sample quality but also diminishes computational demands. Our research adopts this paradigm to maximize the advantages of independently training action modeling and policy modeling.

3 Method

RoLD is characterized by two critical components: 1) A **task-agnostic** yet embodiment-aware autoencoder employed for the uniform modeling of the trajectory latent space, and 2) a visuomotor latent diffusion model that is **task-aware**, applied for multi-task policy modeling. We provide detailed discussions of these two components in sections 3.1 and 3.2 respectively. Subsequently, in section 3.3, we delve into training details that underpin our entire pipeline.

3.1 Latent Trajectory Autoencoder

We aim to design a task-agnostic latent autoencoder for unified action trajectory modeling, namely LAT. The introduction of latent enables the compression of

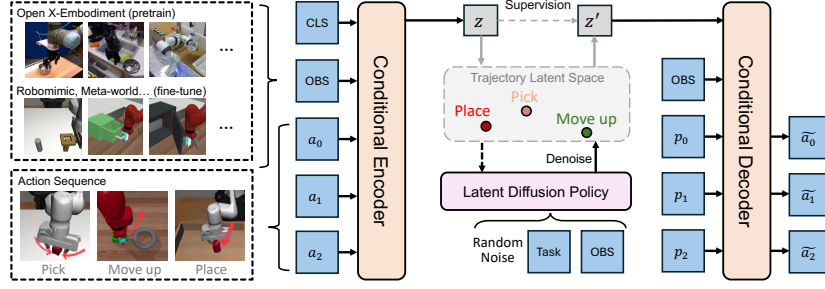


Fig. 1: RoLD comprises two core components: 1) An embodiment-aware yet task-agnostic Latent Autoencoder for Trajectory (LAT) for unified action modeling in a condense latent space, in which each data point is with strong skill-relevant semantics like “placing” and ”picking”. 2) A Latent Diffusion Policy (LDP) that effectively denoises from a sampled noise into a target trajectory latent, conditioned by observations and task indicators for efficient policy modeling. The decoupled architecture of our framework allows us to effectively benefit from large-scale datasets for both action modeling and policy modeling across various embodiments and environments, thereby delivering strong performance on multi-tasking. In this figure, *OBS*, *CLS*, *a* and *p* denote observation, learnable token, action and position embedding respectively.

diverse action sequences of different embodiments under different observations into a concise and semantically rich latent space.

Specifically, we employ a Conditional Variational Autoencoder (CVAE) [44] to encode and reconstruct the action sequences, using observations as condition. The encoder accepts action sequences and image observations as inputs, encoding them into an embodiment-aware latent space denoted as z . The decoder conditions on both the latent features sampled from z and the image observations to reconstruct the original action sequences. The latent trajectory autoencoder is trained to maximize the log-likelihood of action sequences via two loss terms: a reconstruction loss and a KL-penalty towards a standard normal on the learned latent z , formulated as:

$$L_{LAT} = \mathbb{E} z \sim \mathcal{E}(x, o) [\log \mathcal{D}(x|z, o)] + w_{KL} D_{KL}(\mathcal{E}(x, o) || p(z)) \quad (1)$$

where o stands for observation, \mathcal{E} and \mathcal{D} are the conditioned encoder and decoder, and w_{KL} is the weight applied on KL-loss during training.

During the training of the latent trajectory autoencoder, we process image observations from a single timestep and the subsequent h actions, which we refer to as the horizon of the action trajectory. We employ a three-layer transformer encoder to encode the inputs in conjunction with a learnable [CLS] token. The encoded feature corresponding to the [CLS] token is reduced to a dimensionality of $2 \times d_z$, and subsequently partitioned into two components: μ and σ . These

components are used to parameterize the latent variable z , which serves to effectively compress the action sequence and encapsulate it within the context of the given observation. For the decoding process, we concatenate the image features and the low-dimensional proprioceptive features with the latent trajectory variable z . This combined representation is then fed into a series of six transformer encoder layers to establish the conditions for decoding. A transformer decoder, utilizing fixed sine-cosine positional embeddings of length h , reconstructs the action sequences. The decoding phase is critical as it ensures that the latent variable z accurately captures the dynamics of the action trajectories necessary for the reconstruction task.

3.2 Visuomotor Latent Diffusion Policy

By training a latent trajectory autoencoder, we obtain a concise and richly-structured visuomotor latent space, which is task-agnostic. To facilitate multi-task policy modeling, we further employ a latent diffusion policy (LDP) to reconstruct the target latent feature conditioned on task instructions and observations. More specifically, the LAT’s decoder originally accepts sampled noise as input during inference, which mismatches the encoded latent z conditioned with observations during training. Therefore, we aim to design a policy model that can accurately recover the target latent z , conditioned on both observations and task instructions, to enable more precise decoding of action sequences.

Diffusion models, a class of generative models, are architecturally conceived to approximate a target data distribution through an iterative denoising process, starting from a Gaussian noise distribution. These models inherently aim to recover an underlying latent distribution by gradually reversing the diffusion process. Starting from a Gaussian noise x^t , DDPM performs several iterations of denoising to recover the original data gradually:

$$\mathbf{x}^{t-1} = \alpha(\mathbf{x}^t - \gamma\epsilon_\theta(\mathbf{x}^t, t) + \mathcal{N}(0, \sigma^2 I)), \quad (2)$$

where ϵ_θ is a network with parameters θ that predicts the noise and $\mathcal{N}(0, \sigma^2 I)$ is the added Gaussian noise. We use the default settings of α and γ in DDPM. The model ϵ_θ is trained to correctly predict the noise added at each step t :

$$L_{DM} = \mathbb{E}_{x, \epsilon \sim \mathcal{N}(0, 1), t} [\|\epsilon - \epsilon_\theta(x, t)\|_2^2], \quad (3)$$

In our visuomotor latent diffusion policy model, the diffusion model is trained to recover the learned latent feature z introduced in Section 3.1. Consequently, the training objective of our model is adjusted to the following form as in latent diffusion model:

$$L_{LDM} = \mathbb{E}_{\mathcal{E}(x), \epsilon \sim \mathcal{N}(0, 1), t} [\|\epsilon - \epsilon_\theta(z_t, t)\|_2^2], \quad (4)$$

where z_t is obtained from the LAT’s encoder $\mathcal{E}(x)$ during training. During inference, the denoised latent feature z_t is utilized to generate action sequence with LAT’s decoder.

To accurately recover the learned trajectory latent space z and facilitate multi-task policy learning, observations and task instructions are used as conditions in the denoising process. Specifically, we first concatenate textual instruction embeddings, visual embeddings, proprioception embeddings (for downstream tasks), denoising timestep and noise as the input of six layers of self-attention blocks. Consequently, the objective of conditional visuomotor latent diffusion policy model is:

$$L_{LDP} = \mathbb{E}_{\mathcal{E}(x), y, \epsilon \sim \mathcal{N}(0,1), t} [\|\epsilon - \epsilon_{\theta}(z_t, t, \tau_{\theta}(y))\|_2^2], \quad (5)$$

where y denotes the conditions containing visual observations, robot proprioception and task instructions in our experiments. During inference, given current observations and the manipulation task instruction, we first predict a visuomotor latent feature with latent diffusion policy, then an action trajectory is generated with LAT’s decoder condition on the latent feature and observations.

3.3 Model Training

This section outlines the detailed process of our model’s training regimen:

Dataset Preprocessing. To harness the wealth of information in large-scale, diverse robotics datasets for generalized training, we utilize the Open X-Embodiment dataset [34]. This dataset is instrumental for learning the latent space of action sequences and establishing a foundational policy model. The Open X-Embodiment dataset encompasses data from 60 individual real-world datasets, featuring 22 different robotic embodiments and is continually expanding with new data. Given the substantial variability in embodiments, instructions, observations, and action spaces among the sub-datasets, we employ a preprocessing protocol to streamline pre-training.

- Data Filtering. We begin by selectively excluding datasets from our analysis, particularly those pertaining to navigational tasks or involving bi-manual robots, as our focus is on tasks involving single-robot manipulation. Additionally, datasets with ambiguous action formats or erratic action control signals are omitted to enhance training stability. Consequently, our experiments utilize 24 meticulously preprocessed datasets from the Open X-Embodiment dataset suite.
- Data Normalization. We forego traditional normalization techniques on action data. Instead, we first eliminate outliers and then rescale the remaining data to approximately the range of $[-1, 1]$. This normalization is vital for maintaining stability and ensuring compatibility with downstream data, which typically constrains action signals to the same range. For observational data involving multiple camera angles, we employ a strategy of random view selection during each training iteration, promoting robust generalization. We strictly utilize center cropping without distortion to preserve the fidelity of observation-action pairings. Proprioceptive data is not incorporated during pre-training due to its significant heterogeneity across datasets. For subsequent tasks, we maintain the original distribution of action data and replicate the image preprocessing approach from pre-training.

Training Pipeline. Our training commences with the pre-training of the Latent Trajectory Autoencoder (LAT) and Latent Diffusion Policy (LDP) models using the refined Open X-Embodiment dataset. This phase is designed to distill a compact latent space and establish core policy modeling proficiency. Given the critical role of proprioceptive feedback in precise state estimation, we subsequently integrate proprioceptive data into the observational inputs and fine-tune the pre-trained LAT model. The final step involves fine-tuning the pre-trained LDP model, while the LAT encoder provides supervisory guidance and training support to LDP before being discarded during inference.

Other Setups. For visual observation, we employ a non-trainable R3M-ResNet34 [32,15], followed by a trainable three-layer MLP. Concurrently, we use a frozen DistilBERT [40] as our language encoder, ensuring alignment with the R3M framework. The reconstruction of the action sequence in LAT and the latent feature in the diffusion model both utilize an L2 loss function.

4 Experiments

In this section, our objective is to showcase the efficacy of our proposed latent trajectory modeling and visuomotor latent diffusion approach. We begin by detailing the configuration of our experiments in section 4.1. Subsequently, we draw comparisons with three state-of-the-art policy models, DiffusionPolicy [6], ACT [51] and LISA [11] in section 4.2. To further elucidate our detailed design, we have conducted ablation studies and visualizations of the modeled latent action space, which are discussed in sections 4.3 and 4.4, respectively. Finally, we explore the few-shot and scaling capability of RoLD in sections 4.6 and 4.7.

Table 1: Description and statistics of the downstream datasets. #View denotes the number of views of image data, #N stands for the number of training episodes and #L is the average episode length for each task. Statistics for Robomimic are divided into PH/MH for better and worse quality data.

Task	Description	#View	#N	#L
Lift	Object picking	2	200/300	116/209
Can	Pick-n-place	2	200/300	48/104
Square	Picking and assembly	2	200/300	150/269
Assembly	Picking and assembly	1	25	92
Button	Button pressing	1	25	86
Hammer	Picking and hammering	1	25	81
Bin	Pick-n-place	1	25	363
Drawer	Drawer opening	1	25	87

4.1 Experiment settings

Training Details To ensure a fair comparison, we uniformly apply the same learning settings across all methods. We employ a cosine learning rate scheduler with a warm-up period of 1000 steps, peaking at a learning rate of $1e-4$. The training dataset is divided into 95% for training and 5% for validation. The number of epochs is determined based on the convergence of validation loss. Specifically, LAT and LDP are trained for 200 epochs, while it takes 1000 epochs for DiffusionPolicy. This also demonstrates superior training efficiency for separated action modeling and policy modeling. For the pre-training phase, we fix a 10-epoch training on all the methods. All the methods are implemented with an fixed trajectory horizon of $h = 16$ steps considering the average length of training data, i.e., for each step of observation input, we predict the following 16-steps action trajectory, which is aligned to DiffusionPolicy’s and ACT’s setting. We do not specify horizon length for each task to avoid combinatorial explosion of potential horizons across the datasets.

Evaluation setup Our experiments are based on two widely-used simulation benchmarks:

- Robomimic [30] is a standard robot-learning and reinforcement-learning benchmark for manipulation tasks. The training data of Robomimic concludes Proficient Human demonstrations (-PH) and Mixed proficient/non-proficient Human demonstrations (-MH). We separately evaluate the methods trained on the two settings.
- Meta-World [49] is an open-source simulated benchmark for meta-reinforcement learning and multi-task learning. We follow the training data and settings of [29] with five manipulation tasks for multi-task training.

For each benchmark, we use only the available proprioception data as input, excluding environment-specific low-dimensional signals such as target object pose. We set the environment step limit to 400. To balance accuracy and efficiency, we employ a strategy similar to ACT, averaging the first eight actions of the current predicted trajectory with the last eight actions of the previous predicted trajectory as simulator’s input. The reported results are averages from 50 trials with varying seeds. Further details about the datasets can be found in Table 1.

4.2 Comparison with SOTA

We began our evaluation process with an extensive analysis of our technique’s efficiency on multi-task performance, as well as its adaptability to large-scale cross-platform dataset pre-training. The results from multi-task experiments

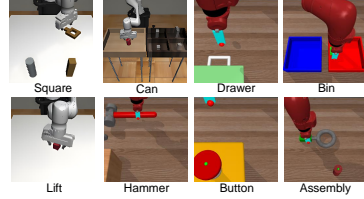


Fig. 2: We conduct experiments on two simulation benchmarks with eight diverse tasks.

conducted on both the Robomimic and Meta-World platforms are outlined in Table 2 and Table 3, respectively.

Proficiency in Multi-Tasking As evidenced in [6], DiffusionPolicy displays a significant superiority in a single-task context; however, it exhibits drawbacks when applied to multi-task policy modeling and vulnerability to overfitting. ACT, employing a similar action compression method to us, consequently achieves enhanced multi-task performance. LISA also fails to perform good on multi-tasking and generalization. In stark contrast, our method consistently outperforms the baseline models on multi-task success rates by a substantial margin of 4% to 10%. We attribute this superior performance to our well-structured trajectory latent space, which allows for better generalization, and our latent diffusion module that ensures stable policy modeling.

Evaluating Pre-training Effectiveness By comparing the results obtained without pre-training and those with pre-training, we observe that ACT only exhibit marginal performance improvement through the pre-training process, while DiffusionPolicy and LISA even appear to deteriorate. By contrast, our model demonstrates an average performance gain of 3.5% from pre-training over the benchmark models. We primarily attribute this significant enhancement to our trajectory latent modeling strategy. This approach effectively condenses intricate embodiment-action combinations into a unified representation, thereby facilitating cross-skill and cross-embodiment generalization.

Table 2: Results on Robomimic benchmark.

	Pretrain	MH			PH			Avg.
		Lift	Can	Square	Lift	Can	Square	
DiffusionPolicy	✗	1.00	0.90	0.12	1.00	0.94	0.22	0.70
ACT	✗	1.00	0.92	0.34	1.00	0.92	0.34	0.75
LISA	✗	1.00	0.78	0.34	1.00	0.82	0.18	0.69
RoLD (ours)	✗	1.00	0.98	0.36	1.00	0.96	0.42	0.79
DiffusionPolicy	✓	1.00	0.78	0.26	1.00	0.82	0.32	0.70
ACT	✓	0.92	0.74	0.32	1.00	0.92	0.40	0.77
LISA	✓	0.88	0.74	0.24	0.92	0.74	0.32	0.64
RoLD (ours)	✓	1.00	0.98	0.48	1.00	1.00	0.56	0.84

In the following sections, we aim to address the following questions:

- Are the design choices in our LAT and LDP essential? 4.3-4.4
- How does the trajectory horizon affect the performance? 4.5
- How does the pre-training perform under few-shot scenarios? 4.6
- Does our model adhere to the scaling laws? 4.7

4.3 Ablation Studies

In this section, we present ablation studies focusing on the key design elements of the Latent Action Trajectory (LAT) and Latent Diffusion Process (LDP)

Table 3: Results on Meta-world benchmark.

	Pretrain	Assembly	Button	Hammer	Bin	Drawer	Avg.
DiffusionPolicy	✗	0.96	0.52	0.96	0.00	1.00	0.69
ACT	✗	0.86	0.80	0.92	0.76	1.00	0.87
LISA	✗	0.98	0.76	0.94	0.78	1.00	0.89
RoLD	✗	0.76	0.96	0.98	0.84	1.00	0.91
DiffusionPolicy	✓	0.92	0.34	0.96	0.00	1.00	0.64
ACT	✓	0.88	0.84	0.84	0.70	1.00	0.85
LISA	✓	1.00	0.78	0.86	0.80	1.00	0.89
RoLD	✓	0.96	1.00	0.86	0.82	1.00	0.93

modules. The results are summarized in Table 4. All experiments were conducted without pre-training.

We first replaced the LDP module with a vanilla transformer encoder with comparable parameters to directly reconstruct the latent variable. The results show a significant decrease in success rates of 18% on Robomimic and 35% on Meta-World, highlighting the critical role of the latent diffusion process in accurate policy modeling.

Regarding LAT, integrating the autoencoder with the task indicator led to a decline in model performance. This decline is interpreted as a corruption of the pure trajectory latent space, underscoring the importance of decoupling action modeling from policy modeling. Furthermore, neglecting observations in LAT resulted in a collapse of the latent space, leading to a deterioration in overall performance even with visual input in LDP. This

collapse can be attributed to the intrinsic relationship between trajectories and the robot’s states for modeling actions and skills. For example, an trajectory involving decreasing values along z-axis might signify a “placing” motion if the robot is in contact with a cube or “inserting” if the robot is handling a frame.

Table 4: Results of ablation experiments on RoLD.

	Robomimic Meta-World	
RoLD	0.79	0.91
- Vanilla policy	0.61	0.53
- LAT w/ task	0.70	0.85
- LAT w/o obs	0.02	0.00

4.4 Latent Space Visualization

To provide an intuitive demonstration of the modeled latent space, we utilized t-SNE [28] to examine our trajectory latent space, as depicted in Figure 3a, and the corresponding space trained with task conditions, illustrated in Figure 3b.

Analysis of the figures clearly demonstrates the effectiveness of our approach in effectively distinguishing between specific **skills** such as “pick” and “assembly”. In contrast, the latent space trained under task-specific conditions tends to group together based on downstream tasks, such as the visual domain, and failed to

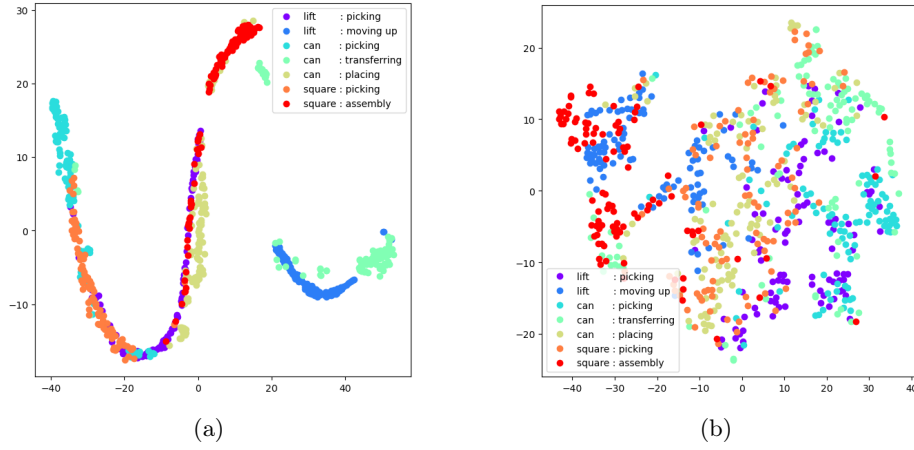


Fig. 3: (a): t-SNE visualization of LAT’s trajectory latent space. (b): t-SNE visualization of latent space whose training is mixed with task condition for policy modeling.

cluster on skills. This tendency can lead to overfitting and reduced performance when faced with multitasking.

4.5 Action Trajectory Horizon

To further investigate the necessity of trajectory modeling, we conducted an experiment on different trajectory horizon sizes. The results are presented in Figure 4.

The figure indicates that as the length of the action trajectory increases, the model’s average performance improves, peaking at a length of 16 steps. However, when the length continues to increase, the model’s performance dramatically declines. We attribute this to the fact that single-step actions or short trajectories typically express weak or no skill-relevant features, making it difficult to construct a unified action space with skill semantics. On the other hand, when the horizon goes larger (24 and 32 steps), more complex movements which can not be clearly encoded into single skills are involved in the latent space modeling process. This complexity can lead to confusion when distinguishing a single skill, resulting in subpar performance.

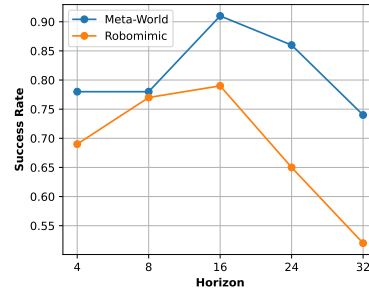


Fig. 4: Averaged success rate on Robomimic and Meta-world of different action trajectory horizon.

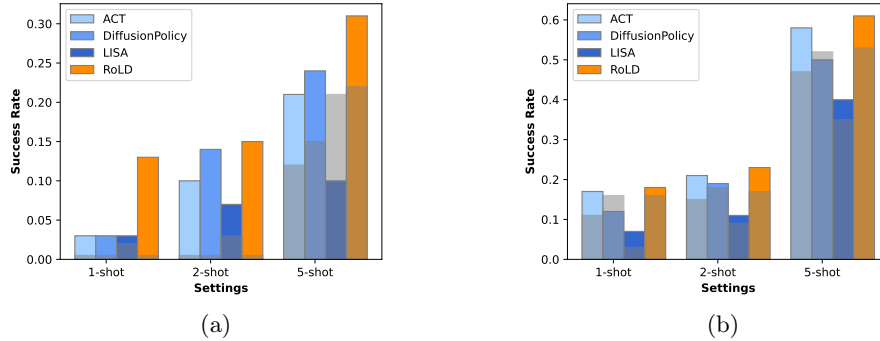


Fig. 5: Few-shot results on (a) Robomimic, and (b) Meta-World.

4.6 Few-shot Learning

To further investigate the efficacy of the pre-training process and evaluate the superiority of our method over the baselines in pre-training, we conducted experiments within few-shot multi-task learning scenarios when compared to existing methods. The experimental setup mirrored that of the primary experiment’s pre-training phase, as outlined in Section 4.1. The results are displayed in Figure 5a and Figure 5b, showcasing averaged multi-task scores. Notably, instances of few-shot results without pre-training are highlighted in grey for comparison.

Upon scrutinizing the results, it becomes evident that our method consistently outperforms the baselines. Particularly noteworthy is our model’s ability to excel in few-shot learning even when the pre-training data comprises real-world cross-robot demonstrations that diverge from the simulation benchmark for the downstream task. This resilience is attributed to the well-structured trajectory latent space cultivated during the pre-training phase within our model. Furthermore, it is observed that pre-training has a detrimental impact on the LISA method, corroborating our primary findings detailed in Section 4.2.

A significant observation is the marginal performance enhancements across all methods when pre-trained on Meta-World. This phenomenon can be attributed to the unique formulation of action data in Meta-World, which solely encompasses position and gripper control signals while omitting rotation information. Consequently, a distribution gap emerges between the pre-training and fine-tuning datasets.

4.7 Scaling

To explore the interplay between model parameter scale and performance, we devised three variants of model sizes and assessed their efficacy on established benchmarks: the Base model, our default configuration; a Medium model featuring a deeper network architecture; and a Large model characterized by both

increased network depth and wider hidden size. Our evaluations on these variants are summarized in Figure 6.

The results indicate a noteworthy performance boost when scaling up from our model with 63 million parameters to one with 103 million parameters. However, further scaling to the Large model with 154 million parameters does not sustain this improvement. We attribute this plateau in performance to the realization that the bottleneck does not lie within the capacity of the policy model itself. Instead, enhancements should be directed towards the perceptual component, specifically the observation features derived from visual encoders with enhanced fine-grained perception capabilities [37,32,29]. Moreover, optimizing a model with such a substantial parameter count may pose challenges due to limited amount of downstream training data.

This finding underscores that achieving a robust visuomotor policy necessitates a synergy of action modeling, policy design enriched with fine-grained perceptual abilities, and access to adequate training data. Mere escalation of model parameters does not consistently translate into improved performance.

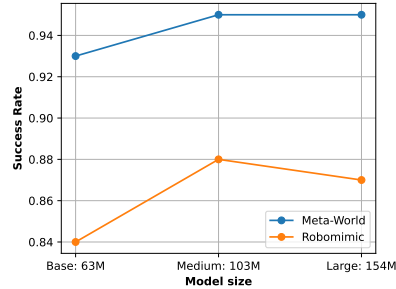


Fig. 6: The averaged success rates of three scales of RoLD on Robomimic and Meta-World benchmark.

5 Limitations and Future Directions

The visuomotor latent diffusion policy introduced in this research has shown promising results, yet several challenges remain that provide opportunities for future exploration and enhancement:

- **Data Normalization** The efficacy of the downstream tasks is notably influenced by the training data distribution. The current normalization method, which scales action signals to a range between -1 and 1 while maintaining their positive characteristics, only partially mitigates the impact of distribution discrepancies encountered during pre-training. To address this, future research could investigate the design of dynamic algorithms capable of autonomously adapting to and harmonizing the training conditions across diverse datasets.
- **Temporal Horizon** The utilization of a fixed latent trajectory horizon has shown to be insufficiently versatile to accommodate the variability inherent in data of different scales and complexities. It is anticipated that the development of more sophisticated algorithms that dynamically adjust to the characteristics of the training data could effectively eliminate this limitation.

- **Computational Efficiency** The iterative denoising steps required by our model, which are common to diffusion-based approaches, impose constraints on the speed of inference. Potential avenue for improvement could involve the integration of more efficient denoising strategies, such as DDIM [16] and DPM-Solver [26], or devising more efficient latent recovery policy.

6 Conclusion

To effectively utilize diverse datasets in robot manipulation tasks and train a more generalized multi-task visuomotor policy, we introduced a two-phase training paradigm. In the first phase, we decoupled action trajectory modeling from policy modeling and constructed a latent trajectory autoencoder for condensed latent action modeling, conditioned by the states of embodiments and observation. In the second phase, we employed a latent diffusion process for stable and efficient policy modeling, conditioned by both observation and task conditions. Experimental results on two widely used multi-task robot learning benchmarks demonstrate the effectiveness of our method in multi-tasking and highlight its capacity to significantly benefit from pre-training.

References

1. Alayrac, J.B., Donahue, J., Luc, P., Miech, A., Barr, I., Hasson, Y., Lenc, K., Mensch, A., Millican, K., Reynolds, M., et al.: Flamingo: a visual language model for few-shot learning. *Advances in Neural Information Processing Systems* **35**, 23716–23736 (2022) [2](#)
2. Brohan, A., Brown, N., Carbajal, J., Chebotar, Y., Chen, X., Choromanski, K., Ding, T., Driess, D., Dubey, A., Finn, C., Florence, P., Fu, C., Arenas, M.G., Gopalakrishnan, K., Han, K., Hausman, K., Herzog, A., Hsu, J., Ichter, B., Irpan, A., Joshi, N., Julian, R., Kalashnikov, D., Kuang, Y., Leal, I., Lee, L., Lee, T.W.E., Levine, S., Lu, Y., Michalewski, H., Mordatch, I., Pertsch, K., Rao, K., Reymann, K., Ryoo, M., Salazar, G., Sanketi, P., Sermanet, P., Singh, J., Singh, A., Soricut, R., Tran, H., Vanhoucke, V., Vuong, Q., Wahid, A., Welker, S., Wohlhart, P., Wu, J., Xia, F., Xiao, T., Xu, P., Xu, S., Yu, T., Zitkovich, B.: RT-2: Vision-Language-Action Models Transfer Web Knowledge to Robotic Control [2](#), [3](#)
3. Brohan, A., Brown, N., Carbajal, J., Chebotar, Y., Dabis, J., Finn, C., Gopalakrishnan, K., Hausman, K., Herzog, A., Hsu, J., Ibarz, J., Ichter, B., Irpan, A., Jackson, T., Jesmonth, S., Joshi, N.J., Julian, R., Kalashnikov, D., Kuang, Y., Leal, I., Lee, K.H., Levine, S., Lu, Y., Malla, U., Manjunath, D., Mordatch, I., Nachum, O., Parada, C., Peralta, J., Perez, E., Pertsch, K., Quiambao, J., Rao, K., Ryoo, M., Salazar, G., Sanketi, P., Sayed, K., Singh, J., Sontakke, S., Stone, A., Tan, C., Tran, H., Vanhoucke, V., Vega, S., Vuong, Q., Xia, F., Xiao, T., Xu, P., Xu, S., Yu, T., Zitkovich, B.: RT-1: Robotics Transformer for Real-World Control at Scale (Dec 2022), *arXiv:2212.06817 [cs]* [2](#), [3](#)
4. Chaumette, F., Hutchinson, S.: Visual servo control. i. basic approaches. *IEEE Robotics & Automation Magazine* **13**(4), 82–90 (2006) [3](#)
5. Chen, L., Lu, K., Rajeswaran, A., Lee, K., Grover, A., Laskin, M., Abbeel, P., Srinivas, A., Mordatch, I.: Decision transformer: Reinforcement learning via sequence

- modeling. *Advances in neural information processing systems* **34**, 15084–15097 (2021) [3](#)
6. Chi, C., Feng, S., Du, Y., Xu, Z., Cousineau, E., Burchfiel, B., Song, S.: Diffusion Policy: Visuomotor Policy Learning via Action Diffusion (Jun 2023), arXiv:2303.04137 [cs] [2](#), [4](#), [8](#), [10](#)
 7. Dasari, S., Ebert, F., Tian, S., Nair, S., Bucher, B., Schmeckpeper, K., Singh, S., Levine, S., Finn, C.: RoboNet: Large-Scale Multi-Robot Learning (Jan 2020), arXiv:1910.11215 [cs] [2](#)
 8. Dosovitskiy, A., Beyer, L., Kolesnikov, A., Weissenborn, D., Zhai, X., Unterthiner, T., Dehghani, M., Minderer, M., Heigold, G., Gelly, S., et al.: An image is worth 16x16 words: Transformers for image recognition at scale. arXiv preprint arXiv:2010.11929 (2020) [2](#)
 9. Du, Y., Yang, M., Dai, B., Dai, H., Nachum, O., Tenenbaum, J.B., Schuurmans, D., Abbeel, P.: Learning Universal Policies via Text-Guided Video Generation (Feb 2023), arXiv:2302.00111 [cs] [2](#), [4](#)
 10. Ebert, F., Yang, Y., Schmeckpeper, K., Bucher, B., Georgakis, G., Daniilidis, K., Finn, C., Levine, S.: Bridge Data: Boosting Generalization of Robotic Skills with Cross-Domain Datasets (Sep 2021), arXiv:2109.13396 [cs] [2](#)
 11. Garg, D., Vaidyanath, S., Kim, K., Song, J., Ermon, S.: Lisa: Learning interpretable skill abstractions from language. *Advances in Neural Information Processing Systems* **35**, 21711–21724 (2022) [2](#), [4](#), [8](#)
 12. Ghadirzadeh, A., Poklukar, P., Kyrki, V., Kragic, D., Björkman, M.: Data-efficient visuomotor policy training using reinforcement learning and generative models. arXiv preprint arXiv:2007.13134 (2020) [3](#)
 13. Goodfellow, I., Pouget-Abadie, J., Mirza, M., Xu, B., Warde-Farley, D., Ozair, S., Courville, A., Bengio, Y.: Generative adversarial nets. *Advances in neural information processing systems* **27** (2014) [4](#)
 14. Guhur, P.L., Chen, S., Pinel, R.G., Tapaswi, M., Laptev, I., Schmid, C.: Instruction-driven history-aware policies for robotic manipulations. In: *Proceedings of The 6th Conference on Robot Learning*. pp. 175–187. PMLR (Mar 2023), iSSN: 2640-3498 [2](#)
 15. He, K., Zhang, X., Ren, S., Sun, J.: Deep residual learning for image recognition. In: *Proceedings of the IEEE conference on computer vision and pattern recognition*. pp. 770–778 (2016) [8](#)
 16. Ho, J., Jain, A., Abbeel, P.: Denoising diffusion probabilistic models. *Advances in neural information processing systems* **33**, 6840–6851 (2020) [4](#), [15](#)
 17. Jang, E., Irpan, A., Khansari, M., Kappler, D., Ebert, F., Lynch, C., Levine, S., Finn, C.: BC-Z: Zero-Shot Task Generalization with Robotic Imitation Learning (Feb 2022), arXiv:2202.02005 [cs] [2](#)
 18. Janner, M., Du, Y., Tenenbaum, J.B., Levine, S.: Planning with Diffusion for Flexible Behavior Synthesis (Dec 2022), arXiv:2205.09991 [cs] [4](#)
 19. Jiang, Y., Gupta, A., Zhang, Z., Wang, G., Dou, Y., Chen, Y., Fei-Fei, L., Anandkumar, A., Zhu, Y., Fan, L.: VIMA: General Robot Manipulation with Multimodal Prompts (May 2023), arXiv:2210.03094 [cs] [2](#), [3](#)
 20. Kingma, D.P., Welling, M.: Auto-encoding variational bayes. arXiv preprint arXiv:1312.6114 (2013) [4](#)
 21. Kumar, A., Singh, A., Ebert, F., Nakamoto, M., Yang, Y., Finn, C., Levine, S.: Pre-Training for Robots: Offline RL Enables Learning New Tasks from a Handful of Trials (Apr 2023), arXiv:2210.05178 [cs] [2](#)

22. Li, J., Li, D., Savarese, S., Hoi, S.: Blip-2: Bootstrapping language-image pre-training with frozen image encoders and large language models. arXiv preprint arXiv:2301.12597 (2023) [2](#)
23. Li, X., Belagali, V., Shang, J., Ryoo, M.S.: Crossway Diffusion: Improving Diffusion-based Visuomotor Policy via Self-supervised Learning (Jul 2023), arXiv:2307.01849 [cs] [2](#), [4](#)
24. Liu, H., Li, C., Wu, Q., Lee, Y.J.: Visual instruction tuning. arXiv preprint arXiv:2304.08485 (2023) [2](#)
25. Liu, Z., Lin, Y., Cao, Y., Hu, H., Wei, Y., Zhang, Z., Lin, S., Guo, B.: Swin transformer: Hierarchical vision transformer using shifted windows. In: Proceedings of the IEEE/CVF international conference on computer vision. pp. 10012–10022 (2021) [2](#)
26. Lu, C., Zhou, Y., Bao, F., Chen, J., Li, C., Zhu, J.: Dpm-solver: A fast ode solver for diffusion probabilistic model sampling in around 10 steps. Advances in Neural Information Processing Systems **35**, 5775–5787 (2022) [15](#)
27. Lynch, C., Sermanet, P.: Language Conditioned Imitation Learning over Unstructured Data (Jul 2021), <http://arxiv.org/abs/2005.07648>, arXiv:2005.07648 [cs] [3](#)
28. Van der Maaten, L., Hinton, G.: Visualizing data using t-sne. Journal of machine learning research **9**(11) (2008) [11](#)
29. Majumdar, A., Yadav, K., Arnaud, S., Ma, Y.J., Chen, C., Silwal, S., Jain, A., Berges, V.P., Abbeel, P., Malik, J., Batra, D., Lin, Y., Maksymets, O., Rajeswaran, A., Meier, F.: Where are we in the search for an artificial visual cortex for embodied intelligence? (2023) [3](#), [9](#), [14](#)
30. Mandlekar, A., Xu, D., Wong, J., Nasiriany, S., Wang, C., Kulkarni, R., Fei-Fei, L., Savarese, S., Zhu, Y., Martín-Martín, R.: What matters in learning from offline human demonstrations for robot manipulation. arXiv preprint arXiv:2108.03298 (2021) [9](#)
31. Mezouar, Y., Chaumette, F.: Path planning for robust image-based control. IEEE transactions on robotics and automation **18**(4), 534–549 (2002) [3](#)
32. Nair, S., Rajeswaran, A., Kumar, V., Finn, C., Gupta, A.: R3M: A Universal Visual Representation for Robot Manipulation (Nov 2022), arXiv:2203.12601 [cs] [3](#), [8](#), [14](#)
33. Ouyang, L., Wu, J., Jiang, X., Almeida, D., Wainwright, C., Mishkin, P., Zhang, C., Agarwal, S., Slama, K., Ray, A., et al.: Training language models to follow instructions with human feedback. Advances in Neural Information Processing Systems **35**, 27730–27744 (2022) [2](#)
34. Padalkar, A., Pooley, A., Jain, A., Bewley, A., Herzog, A., Irpan, A., Khazatsky, A., Rai, A., Singh, A., Brohan, A., Raffin, A., Wahid, A., Burgess-Limerick, B., Kim, B., Scholkopf, B., Ichter, B., Lu, C., Xu, C., Finn, C., Xu, C., Chi, C., Huang, C., Chan, C., Pan, C., Fu, C., Devin, C., Driess, D., Pathak, D., Shah, D., Buchler, D., Kalashnikov, D., Sadigh, D., Johns, E., Ceola, F., Xia, F., Stulp, F., Zhou, G., Sukhatme, G.S., Salhotra, G., Yan, G., Schiavi, G., Su, H., Fang, H.S., Shi, H., Amor, H.B., Christensen, H.I., Furuta, H., Walke, H., Fang, H., Mordatch, I., Radosavovic, I., Leal, I., Liang, J., Kim, J., Peters, J., Schneider, J., Hsu, J., Bohg, J., Bingham, J., Wu, J., Wu, J., Luo, J., Gu, J., Tan, J., Oh, J., Malik, J., Thompson, J., Yang, J., Lim, J.J., Silverio, J., Han, J., Rao, K., Pertsch, K., Hausman, K., Go, K., Gopalakrishnan, K., Goldberg, K., Byrne, K., Oslund, K., Kawaharazuka, K., Zhang, K., Majd, K., Rana, K., Srinivasan, K., Chen, L.Y., Pinto, L., Tan, L., Ott, L., Lee, L., Tomizuka, M., Du, M., Ahn, M., Zhang, M., Ding, M., Srirama, M.K., Sharma, M., Kim, M.J., Kanazawa, N., Hansen, N., Heess, N., Joshi, N.J.,

- Suenderhauf, N., Sanketi, P.R., Wohlhart, P., Xu, P., Sermanet, P., Sundaresan, P., Vuong, Q., Rafailov, R., Tian, R., Doshi, R., Martin-Martín, R., Mendonca, R., Shah, R., Hoque, R., Julian, R., Bustamante, S., Kirmani, S., Levine, S., Moore, S., Bahl, S., Dass, S., Song, S., Xu, S., Haldar, S., Adebola, S., Guist, S., Nasiriany, S., Schaal, S., Welker, S., Tian, S., Dasari, S., Belkhale, S., Osa, T., Harada, T., Matsushima, T., Xiao, T., Yu, T., Ding, T., Davchev, T., Zhao, T.Z., Armstrong, T., Darrell, T., Jain, V., Vanhoucke, V., Zhan, W., Zhou, W., Burgard, W., Chen, X., Wang, X., Zhu, X., Li, X., Lu, Y., Chebotar, Y., Zhou, Y., Zhu, Y., Xu, Y., Wang, Y., Bisk, Y., Cho, Y., Lee, Y., Cui, Y., Wu, Y.h., Tang, Y., Zhu, Y., Li, Y., Iwasawa, Y., Matsuo, Y., Xu, Z., Cui, Z.J.: Open X-Embodiment: Robotic Learning Datasets and RT-X Models **2, 7**
35. Radford, A., Kim, J.W., Hallacy, C., Ramesh, A., Goh, G., Agarwal, S., Sastry, G., Askell, A., Mishkin, P., Clark, J., et al.: Learning transferable visual models from natural language supervision. In: International conference on machine learning. pp. 8748–8763. PMLR (2021) **2**
 36. Radosavovic, I., Shi, B., Fu, L., Goldberg, K., Darrell, T., Malik, J.: Robot Learning with Sensorimotor Pre-training (Jun 2023), <http://arxiv.org/abs/2306.10007>, arXiv:2306.10007 [cs] **2**
 37. Radosavovic, I., Xiao, T., James, S., Abbeel, P., Malik, J., Darrell, T.: Real-world robot learning with masked visual pre-training. In: Conference on Robot Learning. pp. 416–426. PMLR (2023) **3, 14**
 38. Reed, S., Zolna, K., Parisotto, E., Colmenarejo, S.G., Novikov, A., Barth-Maron, G., Gimenez, M., Sulsky, Y., Kay, J., Springenberg, J.T., Eccles, T., Bruce, J., Razavi, A., Edwards, A., Heess, N., Chen, Y., Hadsell, R., Vinyals, O., Bordbar, M., de Freitas, N.: A Generalist Agent (Nov 2022), arXiv:2205.06175 [cs] **2, 3**
 39. Rombach, R., Blattmann, A., Lorenz, D., Esser, P., Ommer, B.: High-resolution image synthesis with latent diffusion models. In: Proceedings of the IEEE/CVF conference on computer vision and pattern recognition. pp. 10684–10695 (2022) **4**
 40. Sanh, V., Debut, L., Chaumond, J., Wolf, T.: Distilbert, a distilled version of bert: smaller, faster, cheaper and lighter. arXiv preprint arXiv:1910.01108 (2019) **8**
 41. Shi, L.X., Sharma, A., Zhao, T.Z., Finn, C.: Waypoint-based imitation learning for robotic manipulation. arXiv preprint arXiv:2307.14326 (2023) **4**
 42. Shridhar, M., Manuelli, L., Fox, D.: CLIPORT: What and Where Pathways for Robotic Manipulation **2, 3**
 43. Siegel, N.Y., Springenberg, J.T., Berkenkamp, F., Abdolmaleki, A., Neunert, M., Lampe, T., Hafner, R., Heess, N., Riedmiller, M.: Keep doing what worked: Behavioral modelling priors for offline reinforcement learning. arXiv preprint arXiv:2002.08396 (2020) **3**
 44. Sohn, K., Lee, H., Yan, X.: Learning structured output representation using deep conditional generative models. Advances in neural information processing systems **28** (2015) **5**
 45. Touvron, H., Lavril, T., Izacard, G., Martinet, X., Lachaux, M.A., Lacroix, T., Rozière, B., Goyal, N., Hambro, E., Azhar, F., et al.: Llama: Open and efficient foundation language models. arXiv preprint arXiv:2302.13971 (2023) **2**
 46. Yang, J., Liu, B., Fu, J., Pan, B., Wu, G., Wang, L.: Spatiotemporal predictive pre-training for robotic motor control. arXiv preprint arXiv:2403.05304 (2024) **3**
 47. Yang, J., Tan, W., Jin, C., Liu, B., Fu, J., Song, R., Wang, L.: Pave the way to grasp anything: Transferring foundation models for universal pick-place robots. arXiv preprint arXiv:2306.05716 (2023) **3**
 48. Yang, J., Sadigh, D., Finn, C.: Polybot: Training One Policy Across Robots While Embracing Variability (Jul 2023), arXiv:2307.03719 [cs] **2**

49. Yu, T., Quillen, D., He, Z., Julian, R., Narayan, A., Shively, H., Bellathur, A., Hausman, K., Finn, C., Levine, S.: Meta-World: A Benchmark and Evaluation for Multi-Task and Meta Reinforcement Learning (Jun 2021), arXiv:1910.10897 [cs, stat] [9](#)
50. Zeng, Y., Zhang, H., Zheng, J., Xia, J., Wei, G., Wei, Y., Zhang, Y., Kong, T.: What matters in training a gpt4-style language model with multimodal inputs? arXiv preprint arXiv:2307.02469 (2023) [2](#)
51. Zhao, T.Z., Kumar, V., Levine, S., Finn, C.: Learning Fine-Grained Bimanual Manipulation with Low-Cost Hardware (Apr 2023), arXiv:2304.13705 [cs] [2](#), [4](#), [8](#)
52. Zhao, W.X., Zhou, K., Li, J., Tang, T., Wang, X., Hou, Y., Min, Y., Zhang, B., Zhang, J., Dong, Z., et al.: A survey of large language models. arXiv preprint arXiv:2303.18223 (2023) [2](#)
53. Zhu, Y., Wang, Z., Merel, J., Rusu, A., Erez, T., Cabi, S., Tunyasuvunakool, S., Kramár, J., Hadsell, R., de Freitas, N., et al.: Reinforcement and imitation learning for diverse visuomotor skills. arXiv preprint arXiv:1802.09564 (2018) [3](#)